Hirosaki Med. J. **60**：63—76, 2009

ORIGINAL ARTICLE

NONHEME-IRON DEPOSITION IN THE HYPOTHALAMO-NEUROHYPOPHYSEAL SYSTEM OF THE RAT BRAIN

Chengtai Li, Saori Odagiri, Reiko Meguro,
Yoshiya Asano and Kazuhiko Shoumura

Abstract The localizations of nonheme-Fe (III) and Fe (II) were studied in the hypothalamo-neurohypophyseal system of the rat brain by light and electron microscopic nonheme iron-histochemistry. Fe (III)-deposit was heavily accumulated in the parvocellular part of the hypothalamic paraventricular nucleus (HPV), where numerous glias were stained. Fe (III)-deposit heavily filled the cytosol and lysosomes of microglia-, oligodendrocyte- and astrocyte-like cells, while neurons contained only a small number of Fe (III)-laden lysosomes. Fine processes of Fe (III)- laden microglia- and oligodendrocyte-like cells closely ensheathed the cell body and proximal dendrites of neurons. Fe (III)-laden astrocyte-like cells tightly enclosed the capillary wall. The magnocellular part of the HPV and the supraoptic nucleus were less intensely stained than the parvocellular part of the HPV. The secretory axon terminals in the outer lamina of the median eminence (ME) and the posterior pituitary including the Herring bodies contained Fe (III)-laden small lysosomes among densely aggregated secretory granules. The secretory axon terminals in the ME were tightly enclosed by heavily Fe (III)-laden processes of tanycyte. The heavily Fe (III)-laden pituicytes and interstitial, pericapillary phagocytes closely approached the secretory axon terminals in the posterior pituitary. Fe (II) was largely localized in the lysosomes throughout the hypothalamo-neurohypophyseal system.

Hirosaki Med. J. **60**：63—76, 2009

Key words: Hypothalamus; Posterior pituitary; Median eminence; Nonheme-iron.

原　著

ラット視床下部・神経下垂体における非ヘム２価（Fe（II））および３価（Fe（III））鉄の局在

李　　成泰　　小田桐紗織　　目黒玲子
浅野義哉　　正村和彦

抄録　ラット視床下部・神経下垂体系の非ヘム鉄(Fe(III)，Fe(II))を光学・電子顕微鏡的組織化学で可視化した．室傍核の小細胞部に集積するFe(III)-陽性グリアが神経細胞を緊密に囲んでいたが，大細胞部と視索上核では，これらの細胞は少数であった．Fe(III)-陽性グリアは細胞基質と水解小体（LS）に強い反応を示した．神経細胞は少数のFe(III)-陽性LSのみを示した．下垂体後葉の軸索終末とヘリング小体（HB）および正中隆起外板の終末は少数のFe(III)-陽性LSを持っていた．後葉細胞の細胞基質とLSはFe(III)-陽性で，終末とHBを緊密に囲んでいた．下垂体後葉と正中隆起外板の毛細血管周囲腔で，Fe(III)-陽性の食細胞が終末に緊密に接触していた．Fe(II)-反応はFe(III)-陽性細胞のLSのみに見られた．これらの所見を内分泌ニューロンの活動と鉄の処理の観点から検討した．

弘前医学　**60**：63—76, 2009

キーワード：視床下部；神経下垂体；正中隆起；非ヘム鉄.

Department of Neuroanatomy, Cell Biology and Histology, Hirosaki University Graduate School of Medicine, Hirosaki 036, Japan
Corresponcence: C. Li
Received for publication, November 28, 2008
Accepted for publication, December 25, 2008

弘前大学医学研究科神経解剖・細胞組織学講座
別刷請求先：李　成泰
平成20年11月28日受付
平成20年12月25日受理

Introduction

The paraventricular nucleus of the hypothalamus (HPV) is a unique structure in the central nervous system, because it has diverse projections on one hand to the median eminence (ME) and posterior lobe of the pituitary gland (posterior pituitary, PP), and on the other hand to the pre-autonomic centers of the brainstem and spinal cord. The former short projections are associated with the pituitary endocrine functions, and the latter long descending projections are associated with the autonomic nervous functions[1]. The cells of origin of these projections and their chemical mediators have been determined by the retrograde transport of tracers and immunohistochemistry for the enzymes involved in the synthesis of transmitters (nitric oxide synthase[2]; tyrosine hydroxylase[3]) and the neurosecretory peptides (oxytocin, 8-arginine vasopressin, somatostatin, methionin-enkephalin, leucine-enkephalin)[4].

The magnocellular and parvocellular divisions of the HPV send short neurosecretory axons to the PP and ME, respectively[1, 5]. The autonomic preganglionic centers of the brainstem and spinal cord receive long descending projections from the cells distributed in both magnocellular and parvocellular divisions of the HPV[1, 6].

Iron is an essential trace metal in living organisms, playing critical roles at the active site of mitochondrial electron transfer proteins (cytochromes) and catalytic enzymes (catalase, peroxidase, aconitase and DNA synthase). Besides these, brain iron is utilized for the neurotransmitter synthesis and degradation and myelination[7, 8]; iron is a coenzyme of tyrosine hydroxylase[9]. Therefore iron is ubiquitous throughout the nervous system. However, particularly dense nonheme- iron accumulation has been known in certain brain regions such as the globus pallidus, substantia nigra pars reticularis, deep cerebellar nuclei and some other structures of the central nervous system[10].

In the hypothalamus, the HPV and the supraoptic nucleus (SO) show prominently intense staining for nonheme Fe (III) as briefly described by Hill and Switzer[11]. This highly localized dense accumulation of nonheme iron in the HPV and SO strongly suggested that it would play a crucial role in the regulation of endocrine and autonomic nervous functions of the HPV and SO. To understand the functional significance of densely accumulated nonheme-iron in the HPV and SO, we studied the topical difference in the accumulation of nonheme-iron, and the cellular and subcellular localization of nonheme-iron in the HPV and SO. We also studied the nonheme iron deposition in the PP and ME, which are one of the major targets of HPV and SO projections.

Materials and Methods

All animal experiments in this study were approved by the Animal Research committee, Hirosaki University, and strictly adhered to the Guidelines for Animal Experimentation, Hirosaki University. Eight to forty weeks old female Wistar rats were supplied from the Institute of Animal Experimentation, Hirosaki University School of Medicine. All animals were anesthetized with pentobarbital sodium (50 mg/kg, i.p.). To visualize tissue nonheme Fe (III) and Fe (II), we used the section- and perfusion-Perls and the perfusion-Turnbull methods[12, 13], respectively.

1. Animal treatments

After thoracotomy, a thin plastic tube was inserted into the ascending aorta from an incision of the left ventricle, and the right auricle was cut. At a rate of 20ml/minute, each animal was perfused with heparinized physiological saline (120ml) followed by the fixatives described below.

2. The fixative for the section-Perls, and perfusion-Perls and -Turnbull methods

The fixative for the section-Perls method consisted of 4% paraformaldehyde (PA) and 0.5% glutaraldehyde (GA) in 0.005 M phosphate buffered saline (PBS, pH 7.4, 1,000ml). The fixative for the perfusion-Perls and -Turnbull methods consisted of 1% potassium ferrocyanide (the perfusion-Perls method) or potassium ferricyanide (the perfusion-Turnbull method), 4% PA, 1% GA in distilled water (1,000 ml). Immediately before the perfusion, the desired pH (1.0) of the fixative was obtained by adding concentrated HCl.

3. Tissue treatment

After the perfusion-fixation, the brain and pituitary gland were taken out and postfixed in 4% PA and 0.5% GA in 0.005 M PBS for 10 min, and sliced at 40-50 μm thickness in 0.005 M PBS on a microslicer (DTK-1,000, Dosaka, Kyoto, Japan) and collected in 0.05 M PBS (pH 7.0). Several pituitary glands fixed for the section-Perls method were embedded in paraffin and cut at 6 μm.

The sections of the tissue fixed for the section-Perls method were incubated in 1% acidic potassium ferrocyanide (pH1.0); then the Fe (III)-reaction product was intensified with 3,3'-diaminobenzidine-4HCl (DAB, Sigma, St Louis, Mo, USA) for light microscopy[14] or with DAB, methenamine silver and gold chloride for electron microscopy[15], according to the procedures recommended by Meguro et al[13].

The sections for light microscopy were mounted on silane-coated glass slides (Matsunami, Osaka, Japan), counter-stained with hematoxylin or thionin in several sections, dehydrated through the graded ethanol series, cleaned in xylene, and cover-slipped. Sections for electron microscopy were, then, postfixed with 1% OsO_4 in PBS (pH 7.4) for 60 min, washed in distilled water, dehydrated through the graded ethanol, treated with propylene oxide and embedded in Epon 812. The ultrathin sections (100 nm thick) were observed under an electron microscope (JEM-2000EX, JEOL, Japan) without counter-staining. In addition, several sections for light microscopy were Nissl-stained.

Results

1. HPV and SO

The histochemical reaction for nonheme Fe (III) was light- microscopically clearly identified by brown amorphous DAB-deposit and electron -microscopically by electron-dense amorphous silver-gold- deposit. The HPV and SO showed an outstanding reaction for Fe (III) among other structures of the hypothalamus. The anterior and medial parts of the parvocellular division of the HPV were intensely stained while the dorsal and lateral parvocellular parts, the posterior part of the magnocellular division and SO were less intensely stained (Fig. 1). In these structures, Fe (III)-deposit strongly stained the cell body and processes (Fig. 2, A-D). On the other hand, most neurons (Fig. 2E) showed only a small number of tiny granular deposits in the cell body. The periventricular zone of HPV was almost unstained (Fig. 1). The HPV and SO were more lightly stained in the young rats (8 weeks old) than in the older (20 and 40 weeks old) rats (Fig. 1).

We classified the heavily Fe (III)-laden glias into astrocyte-, microglia- and oligodendrocyte-like cells (Fig. 2, B-D) according to the light microscopic morphology. Each type of Fe (III)-laden glias mentioned above showed characteristic electron microscopic morphologies for astrocyte-, microglia- and oligodendrocyte-like cells, respectively[16].

The most numerous microglia-like cells showed amoeboid cell shape with a fusiform cell body and irregularly branching, thick processes (Fig. 2C). The oligodendrocyte-like cell were less numerous and characterized by a round to oval cell body, a large, round to oval nucleus with a small nucleolus, and a few thin processes (Fig. 2D). Astrocyte-like cell was smallest in number but was largest in size (Fig. 2A), and usually

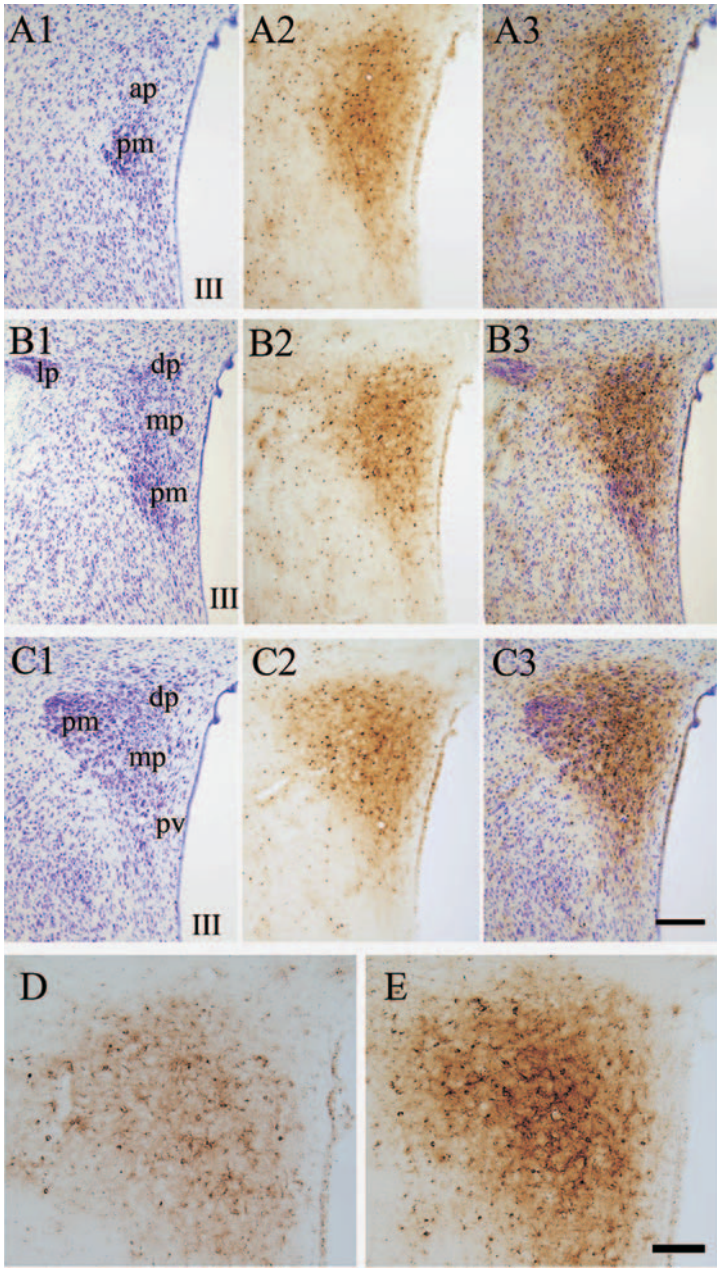

Fig. 1 Comparison of Fe (III)-staining and cytoarchitecture subdivisions of the HPV in 3 serial, 30 μm thick sections (e.g., A1, A2 and A3). A1, B1 and C1 are Nissl stained sections from the brain of a 40 weeks old rat. A2, B2 and C2 are Fe (III)-staining by the section-Perls method. A3, B3 and C3 are the merged photographs of Fe (III) and Nissle staining with thionin (e.g. A3=A1+A2). ap, dp, lp, and mp are anterior, dorsal, lateral and medial parvocellular part, respectively. pm, posterior magnocellular part. Pv, paraventricular zone. III, the third ventricle. D and E, HPV of the 8 weeks and 21 weeks old rat brain, respectively. Section-Perls with DAB intensification on 30μm thick sections. Bar = 100 (D and E) or 200 (A-C) μm.

observed in close vicinity to the capillary wall.

In electron microscopy, iron-laden, microglia-like cells showed a slightly elongated nucleus with a dark karyoplasm, coarse chromatin clumps lining throughout the inner nuclear membrane (Fig. 3A) as described by the previous authors[16]. The cytoplasm was densely filled with iron-deposit including a small number of coarse lysosomes (Fig. 3A). However, cytoplasmic vacuoles were almost unstained (Fig. 3A).

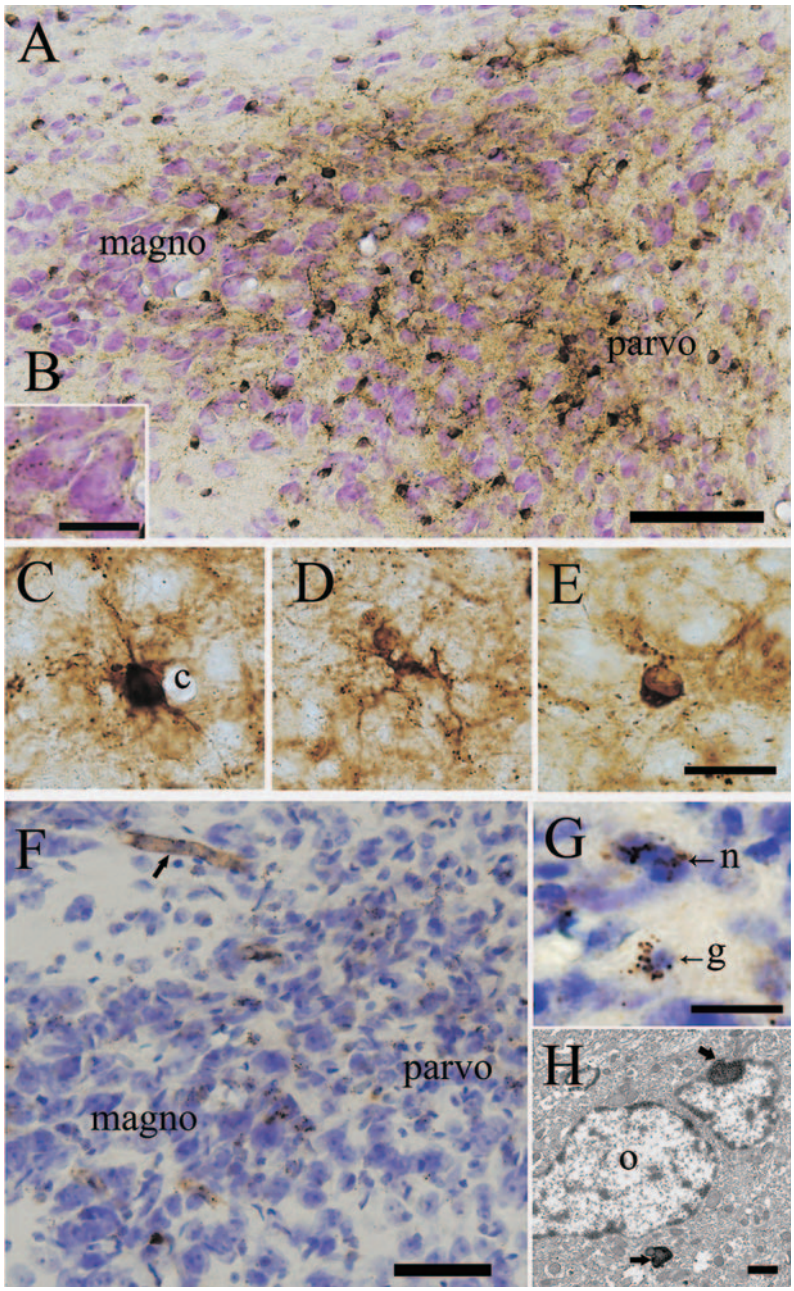

Fig. 2 The HPV stained by the Section-Perls (A-E) or perfusion-Turnbull methods (F and G, 12w old rat) with DAB intensification. A, B, F and G are from sections counter-stained with thionin. A, the adjoining part of the parvocellular (parvo) and magnocellular (magno) parts. B-E show a neuron, an astrocyte-, a microglia- and an oligodendrocyte-like cell, respectively. F, the adjoining part of the parvocellular (parvo) and magnocellular (magno) parts. The arrow indicates a small vessel. G and H indicate Fe (II)-positive grains in a high magnification light microscopy (G) and electron microscopy (H). c, capillary lumen; g, glia-like cell; n, neuron; o, oligodendrocyte-like cell. Bar= 1 (H), 25 (B-E and G), 50 (A and F) and 100 (A) μm.

The oligodendrocyte-like cell had a round to oval nucleus shifted towards one side of the cell body, which contained dense iron-deposit in the cytosol and lysosomes (Fig. 3B). The processes were also densely filled with iron-deposit.

Fe (III)-deposits densely filled the cytosol and small lysosomes of astrocyte-like cells (Fig. 3D), showed a large oval nucleus with a light karyoplasm and were often associated with the capillary wall closely ensheathing the basement

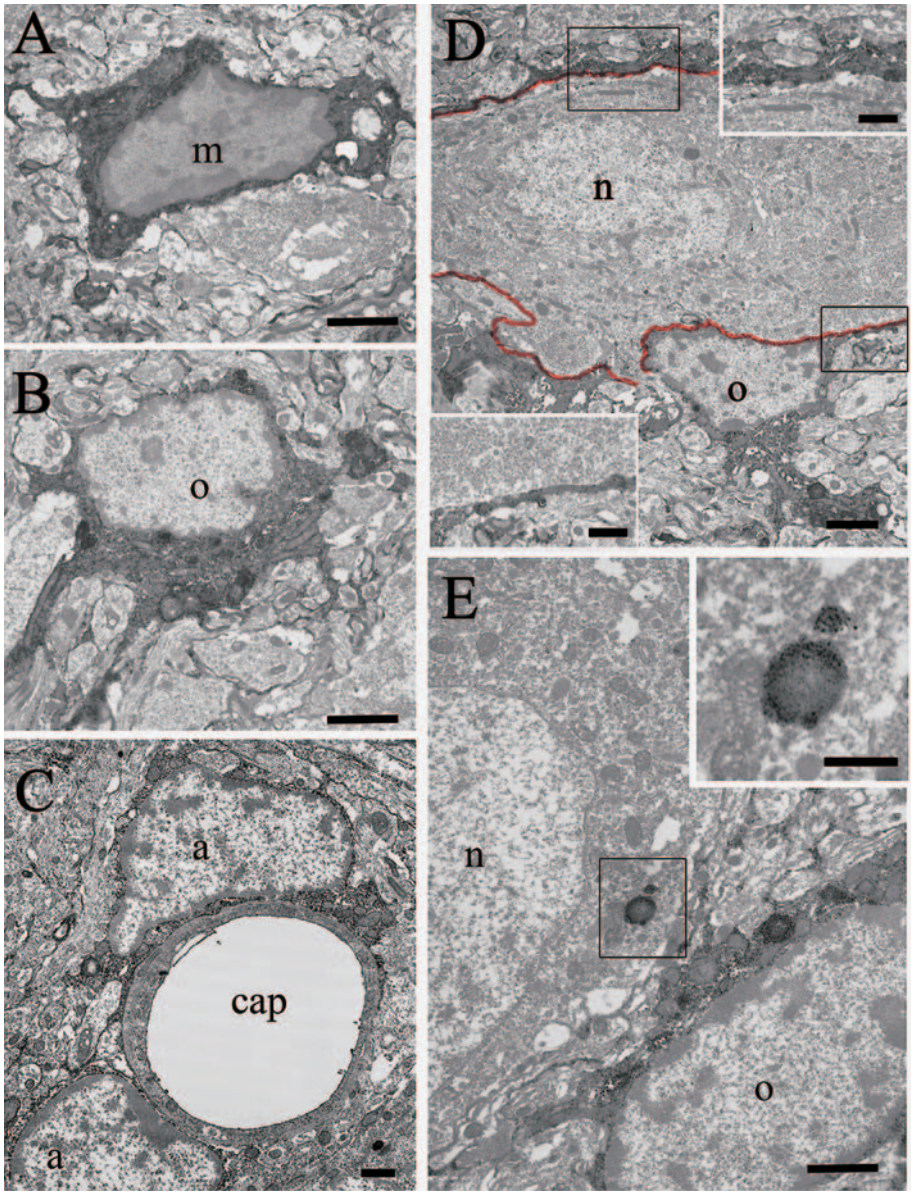

Fig. 3 Electron micrographs of the parvocellular part of the HPV treated by the section-Perls methods with DAB-silver-gold intensification. Twenty-six weeks old rat. A, B and C show Fe (III)-laden microglia-(m), oligodendro- (o) and pericapillary astrocyte- like cell (a), respectively. D and E show neuronal perikarya (n) which are in close proximity with an iron-laden oligodendrocyte-like cell (o) and ensheathed by fine processes of the cell. The neuronal cell membrane is indicated by a red line. Inset photographs in D are a larger magnification to show the close contact between neuronal cell membrane and iron-laden glial process. E also shows iron-laden lysosomes in the neuronal perikaryon (inset) and oligodendrocyte-like cell. cap, capillary lumen. Bar=0.5(E inset), 1 (A-C, E and insets of D), 2 (D) μm.

membrane of the pericyte and endothelial cell (Fig. 3C).

In the parvocellular parts of the HPV, the fine processes of iron-laden glias tightly ensheathed the cell body and proximal dendrites of neurons (Fig. 3D). On the ultrathin sections, the cells of origin of these processes were not clearly determined. However, Fe (III)-laden oligodendroglia- like cell was observed to give off fine processes extending along the the neuronal cell body (Fig. 3, D and E). On the other hand, in the magnocellular parts of the HPV, there was no prominent ensheathing of neurons by Fe (III)-laden glial processes.

In both parvocellular and magnocellular parts of the HPV, the neurons accumulated Fe (III) only in the lysosomes (Fig. 3E). Capillary endothelial cell and pericyte accumulated dense Fe (III)-deposit in a small number of small lysosomes with a small amount of deposit in the cytosol (not shown).

In contrast to the Fe (III) staining, the Fe (II) staining appeared as small granules sparsely scattered in both parvocellular and magnocellular divisions of the HPV (Fig. 2F) and in the SO. By electron microscopy, these granules revealed Fe (II)-deposit in lysosomes in both neurons and glia cells (Fig. 2H).

Interestingly, small blood vessel walls were homogeneously lightly stained for Fe (II) with a small number of Fe (II)-positive coarse or fine granules (Fig. 2E). In electron microscopy, dense Fe (II)-deposit was observed along the adluminal membrane and in the lysosomes of the endothelial cells (not shown).

2. Posterior pituitary: parenchyma

In the parenchyma of the PP, the Fe (III) -positive cellular elements included the pituicyte and microglia (Fig. 4A). Light microscopically, Fe (III)-deposit prominently stained the pituicytes which were characterized by a large, round to oval nucleus and a large cell body (Fig. 4A, inset a). A small number of microglia-like cells were more lightly stained (Fig. 4A, inset b). Iron-deposit lightly stained these cells in 20 weeks old rats (Fig. 4A), and was greatly increased in density in 60 weeks old rats (Fig. 4B).

By electron microscopy, Fe (III)-deposit densely filled the cytosol and /or lysosomes of the pituicytes, but the cytoplasmic lipid droplets which characterize the pituicyte[17, 18] were not stained (Fig. 4, C and E). The pituicytes gave off processes which were in close contact with secretory axon terminals (Fig. 4E). The microglia-like cells contained Fe (III) deposits in the cytosol and/or lysosomes of various sizes (Fig. 4, D and F). Fine processes of microglial cells closely ensheathed secretory axon terminals (Fig. 4D). In addition, the axons, secretory axon terminals and Herring bodies (Fig. 5, A, B and C) contained a small number of small Fe (III)-laden lysosomes.

3. Posterior pituitary: interstitial pericapillary space cells, pericytes and endothelial cells

Heavily Fe (III)-laden cells were observed in the interstitial pericapillary space between the basement membrane lining the parenchyma of the neurohypophysis and that lining the endothelial cell and pericyte (Fig. 5, D and E). There were at least two types of such cells, both of which had a fusiform or elongated cell body with a few thin processes in which cytosol was heavily filled with Fe (III)-deposits (Fig. 5, D and E). One type of such cell had a small, round nucleus containing a small amount of Fe (III) -deposits in the karyoplasm and iron-sparse or -free, large phagosomes of various sizes (Fig. 5D). This type of cell appeared to correspond with the foamy cells, a kind of macrophage derived from the leptomeninges[19]. Occasionally, this type of cell made a close contact with secretory axon terminals which protruded into the perivascular space through the interrupted basement membrane of the pituitary parenchyma (Fig. 5D). These terminals contained a small number of iron-laden small lysosomes. The other type of cell had iron-free elongated, large nucleus and small vacuoles of various sizes (Fig. 5E).

The pericyte and endothelial cells accumulated Fe (III)-deposits in a small number of lysosomes with a small amount of deposit in the cytosol.

In addition, the Fe (II)-deposit was largely localized in the lysosomes throughout the interstitial phagocytic cells, pericytes and capillary endothelial cells.

4. Median eminence

The ME was penetrated by long processes of Fe (III)-laden tanycytes (Fig. 6B). The processes

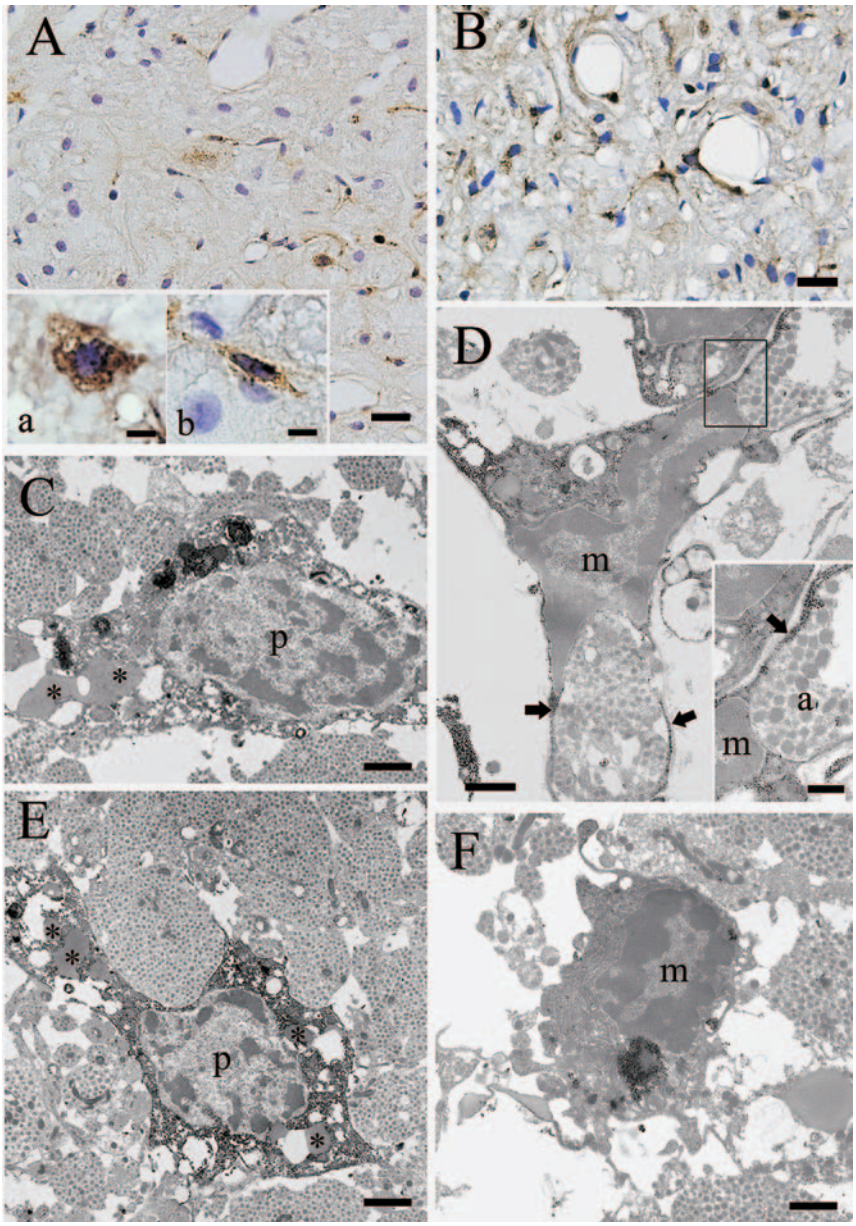

Fig. 4 A and B, Posterior pituitary of 20(A) and 60(B) weeks old rats. Six micrometer thick paraffin-embedded section. The section-Perls method with DAB intensification and hematoxylin counter stain. The left and right insets show a pituicyte and a microglia-like cell, respectively. C-F, the posterior pituitary of 12-15 weeks old rat. Section-Perls method with DAB and silver-gold intensification. C and E show pituicytes which accumulate Fe (III) in the cytosol and lysosomes. Arrows indicate fine processes (of microglia-like cell) ensheathing axon terminals. The inset photograph shows a larger magnification of iron-laden glial process. a, axon terminal; mt, mitochondria. Asterisks, lipid droplets. Bar=0.5 (inset of D), 1 (C-F), 5 (insets of A) and 20 (A and B) μm.

tightly ensheathed the capillary wall in the inner zone of the ME (Fig. 6C), and surrounded the secretory axon terminals containing a small number of Fe (III)-positive lysosomes in the outer zone of the ME. Heavily iron-laden cells were observed in the pericapillary space of the outer zone of the ME (Fig. 6C). These cells were quite comparable to those observed in the posterior pituitary (Fig. 5E).

5. Iron-laden lysosomes in the neuronal perikaryon and secretory axon terminals

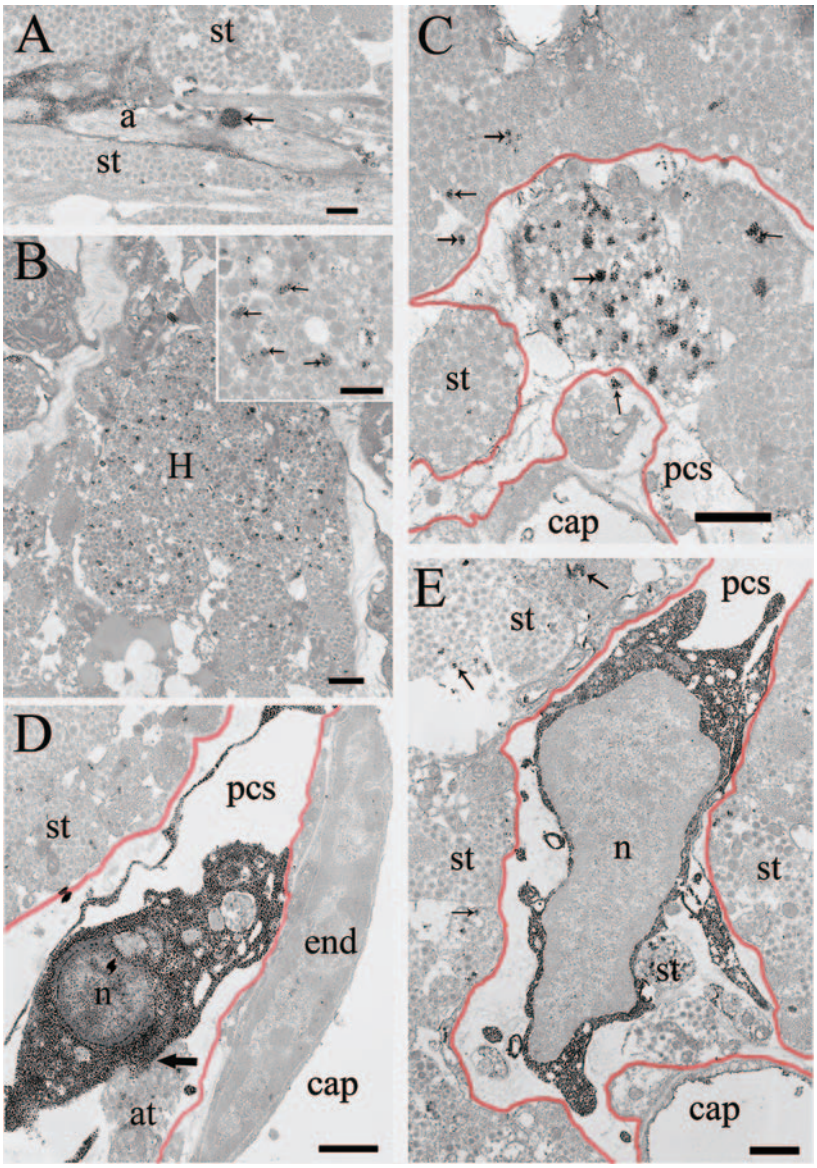

Fig. 5 Electron micrographs of the posterior pituitary. Nine to forty weeks old rats. Section-perls method with DAB and silver-gold intensification. A, a Fe (III)-laden lysosome in an unmyelinated axon (a) of posterior pituitary. At, axon terminal. B, Fe (III)-laden small lysosomes mingled with densely accumulated secretory granules in the Herring body (H). C, an axon terminal containing (at) protruded into the perivascular space (pvs). Arrow indicates Fe (III)-laden small lysosomes. Red line indicates the parenchymal basement membrane. D and E, two types of phagocytic cells in the perivascular space (pvc) which are in close contact (thick arrows) with axon terminals (at). Cap, capillary lumen; end, endothelium; n, nucleu. Bar=500 nm (A and inset of B) and 1(B-E) μm.

The iron-laden lysosomes in the neuronal cell body were much larger (large lysosomes, the diameter was around 500 nm, Figs. 3D and 6A) than those (small lysosomes, the diameter was around 100 nm, Fig. 5) observed in the axon, secretory axon terminals and Herring bodies. In the neuronal cell body, some small lysosomes were observed in close proximity to large lysosomes (Fig. 3E). Furthermore, some large lysosomes appeared to give off small lysosomes (Fig. 6A). These observations suggested the budding of small iron-laden lysosomes for the axonal transport.

Discussion

Here we have demonstrated the localized

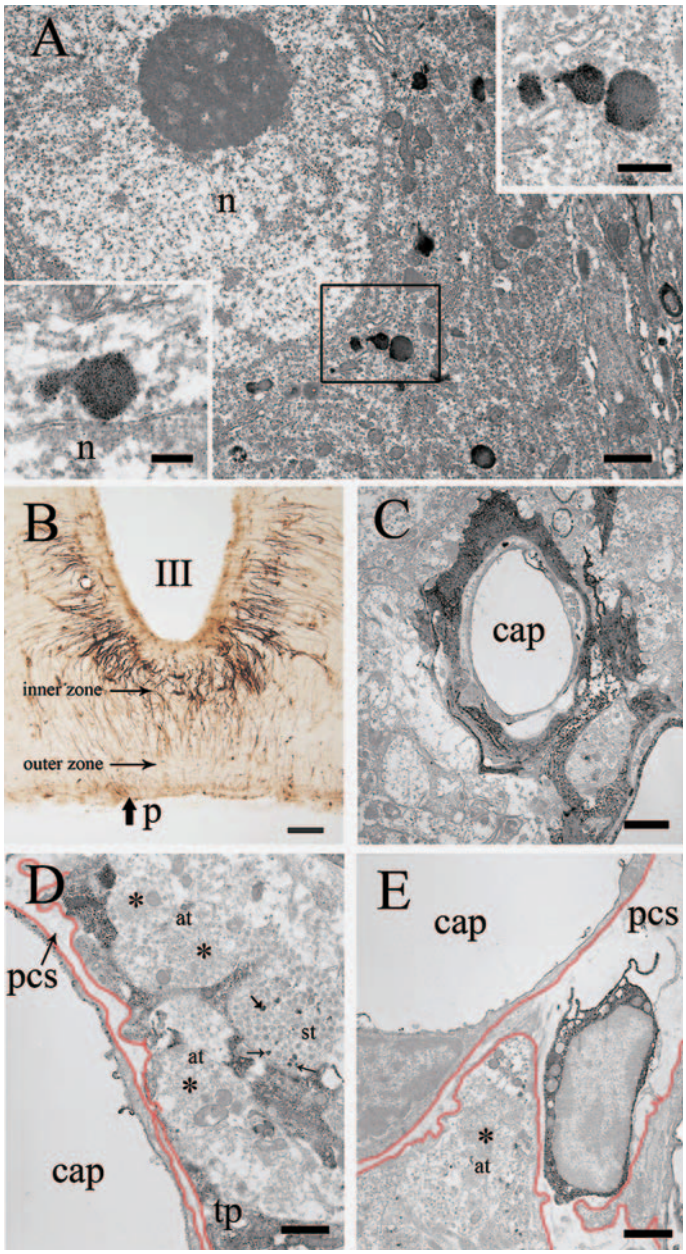

Fig. 6 A, a magnocelluar neuronal perikaryon which contains several Fe (III)- laden lysosomes. Insets show sprouting of small lysosomes from a large one. Twelve weeks old rat. B, light micrograph of the ME stained by the section-Perls method with DAB intensification. Dark brown threads are processes of tanycytes which extend as far as the pial surface (p). Forty weeks old rat. C, capillary in the inner zone of the ME tightly surrounded by a Fe (III)-laden processes of a tanycyte. Red lines indicate basement membranes. Twelve weeks old rat. D, secretory axon terminals (st) ensheathed by a Fe (III)-laden process of tanycyte in the outer zone of the ME. Forty weeks old rat. Asterisks indicate secretory axon terminals containing mostly "synaptoid" structures which are considered to represent the membranes recaptured[40]. E, a heavily Fe (III)-laden, pericapillary phagocytic cell in the outer zone of the ME. Forty weeks old rat. cap, capillary lumen; end, endothelium; p, pial surface; tp, tanycyte process; pcs, pericapillary space. Arrows indicate small Fe (III)-laden lysosome. Bar=200 nm (inset of A), 1 (A, D and E) μm, 2 (C) μm and 50 (B) μm.

cellular and subcellular depositions of nonheme iron in the hypothalamo-neurohypophyseal system of the rat. Fe (III) was the major form of nonheme iron throughout the system, being localized in both cytosol and lysosomes. On the other hand, Fe (II) was detectable only in lysosomes. This is in agreement with the previous study of our own in the rat spleen[20], in which

we observed Fe (II) only in lysosomes while both cytosol and lysosome contained Fe (III). Fe (III) is very probably in the form of iron-storage; ferritin in the cytosol and lysosomes, and hemosiderin in the lysosomes. The presence of nonheme iron in the reduced form in the lysosomes is due to the reduction of Fe (III) by undetermined reducing agents or reductase to release soluble Fe (II) into the cytosol[20].

1. Some possible significance of nonheme-iron accumulation in the HPV and SO

The presence of numerous heavily iron-laden glias in the parvocellular division of the HPV is of particular interest. Fe (III)-reaction was particularly intense in the anterior, and medial parts of the parvocellular part, and less intense in other parts of the parvocellular division and through the magnocellular division of the HPV and the SO.

The iron-rich parts of the parvocellular division appeared to correspond with those parts which project to the median eminence[5], where corticotrophin releasing factor is secreted from the secretory axon terminals into the pericapillary space[21]. These neurons also send descending fibers to the brainstem and spinal cord regions that are intimately related to the autonomic functions[1, 22].

The observations by the previous and present authors suggest that iron-laden glial processes which tightly ensheathed the cell body of parvocellular neurons play important roles on one hand as a source of iron required by the neurons for their metabolism and on the other hand as a barrier to isolate them from the nitric oxide (NO) -rich environment, as considered below.

Firstly, the activity of the parvocellular neurons is controlled by the strong GABAergic inhibitory inputs from the diffusely distributed local neurons[23]. Recently, GABA transaminase was demonstrated to have an iron-sulfur cluster at the center of GABA transaminase dimmer[24]. This enzyme is synthesized in the postsynaptic neurons and astrocytes[25] and plays an essential role for the degradation of GABA. Therefore, the neurons and astrocytes of the parvocellular region should have a strong demand for the iron supply from the surrounding glias to maintain the regulated neuronal activity.

Secondarily, many neurons of the magnocellular division are immuno- positive for the neuronal nitric oxide-synthase (NOS)[2] which catalyzes the generation of gaseous, membrane-permeable nitric oxide (NO). NO potentiates the GABAergic inhibitory inputs to the magnocellular neurons, controlling their spinal and neurohypophyseal outputs[26, 27].

On the other hand, NOS-positive neurons are only sparsely distributed in the parvocellular region[2], suggesting that the neuronal activity of that region does not depend so much on NO as does the magnocellular region. Therefore, to prevent NO-mediated over activation of GABAergic inhibitory inputs, the neurons of the parvocellular region need to be tightly enclosed with iron-rich glial processes, because iron can reversibly bind to NO[28] and because the neurons of the nearby magnocellular region generate diffusible NO. Iron is also essential for the neurons of the magnocellular region of the HPV because heme-containing cofactor is required for the synthesis of NOS[29, 30] and its expression is enhanced by high iron diet[31].

Nonheme Fe (III) in the cytosol of iron-laden glias is most likely in the form of ferritin, because a strong immuno-reactivity for ferritin has been demonstrated in the cytoplasm of microglias and oligodendrocytes of the rat brain[32, 33].

Ferritin immunoreactivity has been also demonstrated in the neurons of the magnocellular part of the HPV and those of the SO of the rat brain[34]. The ferritin immunoreactivity and expression of transferrin receptor increased after 8 days water deprivation[34]. These findings strongly suggest that iron uptake by neurons

increases in the response to stressfull conditions. Indeed, water deprivation, salt loading, immobilization, and swim stress, induce an increased NOS expression[27] which requires iron for NOS synthesis, besides increased secretion of vasopressin and ACTH.

Increased accumulation of nonheme iron in the HPV and SO in the older rat brains as suggested by the present result is important, because it can catalyze the generation of highly cytotoxic hydroxyl-radicals during Haber-Weiss and Fenton reactions in the presence of superoxide and hydrogen peroxide[35, 13]. This could be one of the possible causes for a significant decrease in the number of oxytocin-like, vasopressin-like, and neurophysin-like immunoreactive neurons in the rat paraventricular nucleus during aging[36].

2. Nonheme-iron accumulation in phagocytic cells of the neurohypophysis

Phagocytic processing of secretory axon terminals has been described as a key function in the regulation of oxytocin and vasopressin secretion[37]. The Herring body and large secretory axon terminals contained small, round, iron-laden lysosomes among densely packed secretory granules. Furthermore, the pituicyte and microglia of the parenchyma and the pericapillary phagocytic cells of the interstitium showed dense accumulation of nonheme iron. Moreover, there were increased numbers of heavily iron-laden glias in the parenchyma of older rats. These findings suggested that iron accumulation in these cells was largely caused by phagocytic processing of secretory axon terminals which contain iron-laden lysosomes among densely aggregated secretory granules. The phagocytic processing of the secretory axon terminals benefits the neurons of the HPV and SO, providing a route for the nonheme-iron excretion.

Early histopathologic studies on the postmortem specimens noted a gradual increase in the Fe (III) deposition in the human pituitary gland with age[38]. Iron deposition was more prominent in the anterior pituitary and was associated with increased connective tissue (fibrosis). Iron deposition also occurred in the PP, but not always associated with connective tissue increase. Recent MRI studies of the human pituitary gland support these findings[39]. The present observations in the rat suggested that the increased nonheme iron deposition in the human PP with age is largely due to the increased iron deposition in the parenchymal and interstitial phagocytic cells. The increased iron accumulation in the phagocytic cells of the PP would deteriorate the phagocytic control of neurosecretion.

Summary

Nonheme iron (Fe (III) and Fe (II)) histochemistry in the paraventricular-neurohypophyseal system of the rat demonstrated iron deposits in the following structures. 1) Parvocellular part of the HPV contained strongly Fe (III)-laden glias, which tightly surrounded the cell body and proximal dendrites of neurons. 2) Magnocellular part of the HPV and SO contained a smaller number of Fe (III)-laden glias, and, in contrast to the parvocellular part, the cell body and dendrites of neurons were not enclosed by iron-laden glial processes. 3) Neurons of parvocellular and magnocellular parts of HPC stored Fe (III) only in lysosomes. 4) Secretory axon terminals in the ME and posterior pituitary, and Herring body contained a small number of Fe (III)-laden lysosomes among densely segregated secretory granules. 5) Heavily iron-laden pituicytes and pericapillary phagocyte closely approached the secretory terminals in the posterior pituitary. 6) Fe (III)-laden glias and pituicytes apparently increased in number with age. 7) In contrast to Fe (III), Fe (II) was strictly localized in lysosomes. The iron deposition along the paraventricular-neurohypophyseal system was

considered to be involved in the regulation of HPV neuronal activity through the synthesis of iron-dependent GABA-transaminase and NOS, and in the excretion of excess iron from the system through phagocytosis, by pituicytes and pericapillary phagocytes, of axon terminals containing iron-laden lysosomes.

References

1) Swanson LW, Kuypers HGJM. The paraventricular nucleus of the hypothalamus: cytoarchitectonic subdivisions and organization of projections to the pituitary, dorsal vagal complex, and spinal cord as demonstrated by retrograde fluorescence double-labeling methods. J Comp Neurol 1980;194:555-70.

2) Nylén A, Skagerberg G, Alm Per, Larsson B, Holqvist B, Anderson K-E. Nitric oxide synthase in the hypothalamic paraventricular nucleus of the female rat; organization of spinal projections and coexistence with oxytocin or vasopressin. Brain Res 2001;908:10-24.

3) Swanson LW, Sawchenko PE, Bérod A, Hartman BK, Helle KB,Vanorden DE. An immunohistochemical study of the organization of catecholaminergic cells and terminal fields in the paraventricular and supraoptic nuclei of the hypothalamus. J Comp Neurol 1981;196(2):271-85.

4) Sawchenko PE, Swanson LW. Immunohistochemical identification of neurons in the paraventricular nucleus of the hypothalamus that project to the medulla or to the spinal cord in the rat. J Comp Neurol 1982;205:260-72.

5) Wiegand SJ, Price JL. Cells of origin of the afferent fibers to the median eminence in the rat. J Com Neurol 1980;192(1):1-19.

6) Swanson LW, Sawchenko PE. Paraventricular nucleus: a site for the integration of neuroendocrine and autonomic mechanisms. Neuroendocrinology 1980;31:410-17.

7) Beard J. Iron deficiency alters brain development and functioning. J Nutur 2003;133(5 Suppl 1):1468S-72S.

8) Connor JR, Menzies SL. Relationship of iron to oligodendrocytes and myelination. Glia 1996;17(2):83-93.

9) Wigglesworth J.M and Baum H. Iron dependent enzymes in the brain. In: Youdim M. B. H, editors. Brain Iron: Neurochemical and Behavioural Aspects. London: Taylor and Francis; 1988.p.25-66.

10) Morris CM, Candy JM, Oakley AE, Bloxham CA, Edwardson JA. Histochemical distribution of non-haem iron in the human brain. Acta Anat (Basel) 1992;144(3):235-57.

11) Hill JM, Switzer III RC, The regional distribution and cellular localization of iron in the rat brain. Neuroscience 1984;11:595-603.

12) Meguro R, Asano Y, Iwatsuki H, Shoumura K. Perfusion-Perls and -Turnbull methods supplemented by DAB intensification for nonheme iron histochemistry: demonstration of the superior sensitivity of the methods in the liver, spleen, and stomach of the rat. Histochem Cell Biol 2003;120(1):73-82.

13) Meguro R, Asano Y, Odagiri S, Li C, Iwatsuki H, Shoumura K. Nonheme-iron histochemistry for light and electron microscopy: a historical, theoretical and technical review. Arch Histol Cytol 2007;70(1):1-19.

14) Nguyen-Legros J, Cesaro P, Berger B, Alvarez C. Demonstration of double-labelled branched neurons in the CNS of the rat by retrograde axonal transport of iron-dextran complex and HRP. An application to epoxy-embedded material. Folia Morphol (Praha) 1980;28(3):246-50.

15) Teclemariam-Mesbah R, Wortel J, Romijn HJ, Buijs RM. A simple silver-gold intensification procedure for double DAB labeling studies in electron microscopy. J Histochem Cytochem 1997;45(4):619-21.

16) Pannese E. Neurocytology, Fine Structure of Neurons, Nerve Processes, and Neuroglial Cells. Georg Thieme Verlag, Stuttgart, New-York, 1994.

17) Takei Y, Seyama S, Pearl GS, Tindall GT. Ultrastructural study of the human neurohypophysis. II. Cellular elements of neural parenchyma, the pituicytes. Cell Tissue Res 1980;205(2):273-87.

18) Olivieri-Sangiacomo C. Ultrastructural features of pituicytes in the neural lobe of adult rats. The

cytoplasm. Experientia 1973;29(12):1538-9.

19) Jones EG. On the mode of entry of blood vessels into the cerebral cortex. J Anat 1970;106:507-20.

20) Meguro R, Asano Y, Odagiri S, Li C, Iwatsuki H, Shoumura K. The presence of ferric and ferrous iron in the nonheme iron store of resident macrophages in different tissues and organs: histochemical demonstrations by the perfusion-Perls and -Turnbull methods in the rat. Arch Histol Cytol 2005;68(3):171-83.

21) Sawchenko PE, Swanson LW, Vale WW. Co-expression of corticotrophin-releasing factor and vasopressin immunoreactivity in parvocellular neurosecretory neurons of the adrenalectomized rat. Proc Nat Acad Sci 1984;81:1883-7.

22) Stern JE. Electrophysiological and morphological properties of pre-autonomic neurons in the rat hypothalamic paraventricular nucleus. J Physiol 2001;562(3):725-44.

23) Miklós IH, Kovács KJ. GABAergic innervation of corticotropin-releasing hormone (CRH) -secreting parvocellular neurons and its plasticity as demonstrated by quantitative immunoelectron microscopy. Neuroscience 2002;113(3):581-9.

24) Storici P, De Biase D, Bossa F, Bruno S, Mozzarelli A, Peneff C, Silverman RB, Schirmer T. Structures of gamma-aminobutyric acid (GABA) aminotransferase, a pyridoxal 5'-phosphate, and [2Fe-2S] cluster-containing enzyme, complexed with gamma-ethynyl-GABA and with the antiepilepsy drug vigabatrin. J Biol Chem 2004;279(1):363-73.

25) Kugler P. In situ measurements of enzyme activities in the brain. Histochem J 1993;25(5):329-38.

26) Li D-P, Chen S-R, Finnegan TF, Pan H-L. Signalling pathway of nitric oxide in synaptic GABA release in the rat paraventricular nucleus. J Physiol 2003;554:100-10.

27) Kadekaro M, Nitric oxide modulation of the hypothalamo- neurohypophyseal system. Braz J Med Biol Res 2004;37:441-50.

28) Cooper CE. Nitric oxide and iron proteins. Biochim Biophys Acta 1999;1411:290-309.

29) Kim S, Ponka P. Role of nitric oxide in cellular iron metabolism. Biometals 2003;16:125-35.

30) Porasuphatana S, Tsai P, Rosen GM. The generation of free radicals by nitric oxide synthase. Comp Biochem Physiol C Toxicol Pharmacol 2003;134:281-9.

31) Kim MJ, Kim HK, Chung JH, Lim BO, Yamada K, Lim Y, Kang SA. Increased expression of hypothalamic NADPH-diaphorase neurons in mice with iron supplement. Biosci Biotechnol Biochem 2005;69(10):1978-81.

32) Kaneko Y, Kitamoto T, Takeishi J, Yamaguchi K. Ferritin immunohistochemistry as a marker for microglia. Acta Neuropathol 1989;79:129-36.

33) Cheepsunthorn P, Palmer C, Connor JR. Cellular distribution of ferritin subunits in postnaral rat brain. J Comp Neurol 1998;400:73-86.

34) Tokunaga A, Ono K, Ono T, Ogawa M: Magnocellular neurosecretory neurons with ferritin-like immunoreactivity in the hypothalamic supraoptic and paraventricular nuclei of the rat. Brain Res 1992;597:170-5.

35) Halliwell B, Gutteridge JMC: Free radicals in biology and medicine. 4thed, Oxford University Press, Oxford-New York, 2007.

36) Calzá L, Giardino L, Velardo A, Battistini N, Marrama P. Influence of aging on the neurochemical organization of the rat paraventricular nucleus. J Chem Neuroanat 1990;3(3):215-31.

37) Pow DV, Perry Vh, Morris JF, Gordon S, Microglia in the neurohypophysis associate with and endocytose terminal portions of neurosecretory neurons. Neuroscience 1989;33:567-78.

38) Greenberg SR, The pathogenesis of hypophyseal fibrosis in aging: its relationship to tissue iron deposition. J Gerontol 1975;30:531-8.

39) Fujisawa I, Morikawa M, Nakano Y, Konishi J. Hemochromatosis of the pituitary gland: MR imaging. Radiology 1988;168(1):213-4.

40) Seyama S, Pearl GS, Takei Y. Ultrastructural study of the human neurohypophysis. I. Neurosecretory axons and their dilatations in the pars nervosa. Cell Tissue Res 1980;205(2):253-71.